Original Article

MOLECULAR METABOLISM

Enteroendocrine-derived glucagon-like peptide-2 controls intestinal amino acid transport

Jennifer Lee [1,2], Jacqueline Koehler [1,2], Bernardo Yusta [1,2], Jasmine Bahrami [1,2], Dianne Matthews [1,2], Mahroukh Rafii [1,2], Paul B. Pencharz [1,2], Daniel J. Drucker [1,2,*]

ABSTRACT

Objective: Glucagon-like peptide-2 (GLP-2) is co-secreted with GLP-1 from gut endocrine cells, and both peptides act as growth factors to expand the surface area of the mucosal epithelium. Notably, GLP-2 also enhances glucose and lipid transport in enterocytes; however, its actions on control of amino acid (AA) transport remain unclear. Here we examined the mechanisms linking gain and loss of GLP-2 receptor (GLP-2R) signaling to control of intestinal amino acid absorption in mice.

Methods: Absorption, transport, and clearance of essential AAs, specifically lysine, were measured *in vivo* by Liquid Chromatography triple quadrupole Mass Spectrometry (LC-MS/MS) and *ex vivo* with Ussing chambers using intestinal preparations from *Glp2r*$^{+/+}$ and *Glp2r*$^{-/-}$ mice. Immunoblotting determined jejunal levels of protein components of signaling pathways (PI3K-AKT, and mTORC1-pS6-p4E-BP1) following administration of GLP-2, protein gavage, and rapamycin to fasted *Glp2r*$^{+/+}$ and *Glp2r*$^{-/-}$ mice. Expression of AA transporters from full thickness jejunum and 4F2hc from brush border membrane vesicles (BBMVs) was measured by real-time PCR and immunoblotting, respectively.

Results: Acute administration of GLP-2 increased basal AA absorption *in vivo* and augmented basal lysine transport *ex vivo*. GLP-2-stimulated lysine transport was attenuated by co-incubation with wortmannin, rapamycin, or tetrodotoxin *ex vivo*. Phosphorylation of mTORC1 effector proteins S6 and 4E-BP1 was significantly increased in wild-type mice in response to GLP-2 alone, or when co-administered with protein gavage, and abolished following oral gavage of rapamycin. In contrast, activation of GLP-1R signaling did not enhance S6 phosphorylation. Disruption of GLP-2 action in *Glp2r*$^{-/-}$ mice reduced lysine transport *ex vivo* and attenuated the phosphorylation of S6 and 4E-BP1 in response to oral protein. Moreover, the expression of cationic AA transporter *slc7a9* in response to refeeding, and the abundance of 4F2hc in BBMVs following protein gavage, was significantly attenuated in *Glp2r*$^{-/-}$ mice.

Conclusions: These findings reveal an important role for GLP-2R signaling in the physiological and pharmacological control of enteral amino acid sensing and assimilation, defining an enteroendocrine cell-enterocyte axis for optimal energy absorption.

Keywords GLP-2; GLP-1; Amino acid absorption; Rapamycin; Gut peptides

1. INTRODUCTION

The intestine is a highly dynamic organ that withstands insults posed by exposure to the external environment, while maintaining the capacity for nutrient digestion and absorption to maintain energy homeostasis. The principal differentiated cell types within the gut epithelium, namely enterocytes, Paneth cells, goblet cells, and enteroendocrine cells exhibit specialized functions that contribute to mucosal defense and barrier integrity, while ensuring the capacity for optimal nutrient absorption. Disruption of the integrated function of these cell types, and their supporting networks comprised of immune cells and enteric neurons, often compromises the integrity and absorptive function of the gut, leading to clinical disorders characterized by loss of energy assimilation and weight loss.

Genetic and evolutionary pressure to sustain nutrient absorption and meet energy requirements under circumstances characterized by famine, or malabsorption secondary to gut pathogens, has favored development of a highly efficient intestinal network that maximizes mucosal exposure to and absorption of nutrients. Indeed, the control of gut motility and the anatomical organization of enterocytes within villous structures associated with microvilli optimize maximal interaction of digested nutrients with absorptive gut surface area, thereby

[1]Department of Medicine, University of Toronto, Canada [2]Lunenfeld-Tanenbaum Research Institute, Mt. Sinai Hospital, Toronto, ON M5G 1X5, Canada

*Corresponding author. Lunenfeld-Tanenbaum Research Institute, Mt. Sinai Hospital, 600 University Ave, Toronto, ON M5G 1X5, Canada. Fax: +1 416 361 2669. E-mail: drucker@lunenfeld.ca (D.J. Drucker).

Abbreviations: mTORC1, mechanistic target of rapamycin complex 1; 4E-BP1, eukaryotic translation initiation factor 4E (eIF4e)-binding protein 1; GLP-1, Glucagon-like peptide-1; AA, amino acid; LC-MS/MS, liquid chromatography triple quadrupole mass spectrometry; GLP-2R, GLP-2 receptor; S6K1, 70 kDa ribosomal protein S6 kinase 1; GLP-2, glucagon-like peptide-2; EECs, enteroendocrine cells; PGDP, proglucagon-derived peptides; EAA, essential amino acid; BBMV, brush border membrane vesicles; ENS, enteric nervous system

Received January 6, 2017 • Accepted January 11, 2017 • Available online 17 January 2017

http://dx.doi.org/10.1016/j.molmet.2017.01.005

enabling highly efficient absorption of available ingested energy. Not surprisingly perhaps, the recent shift away from evolutionary pressures associated with energy deprivation to the current environment characterized by energy surplus and the development of obesity reflects in part a highly efficient intestinal system that has evolved over time to favor maximal absorption of available nutrients.

Among the specialized cell types localized to the gut epithelium, enteroendocrine cells (EECs) have evolved in part to control the efficiency of nutrient absorption through secretion of specialized peptide hormones that act in an autocrine, paracrine, or endocrine manner to transmit signals related to nutrient availability [1]. Although dozens of specialized EEC subtypes that express distinct peptide families have been identified [2–4], considerable attention has been focused on the activity of peptides secreted from enteroendocrine L cells, predominantly the proglucagon-derived peptides (PGDPs) [5,6]. The intestinal PGDPs, notably glucagon-like peptide-1 (GLP-1) and oxyntomodulin, exhibit robust actions controlling gut motility, intestinal lipoprotein production, appetite, islet function, and glucose homeostasis [7]; collectively, these attributes have fostered the development of GLP-1 receptor agonists and dipeptidyl peptidase-4 (DPP-4) inhibitors for the treatment of type 2 diabetes [5,6].

Enteroendocrine L cells also co-secrete glicentin and glucagon-like peptide-2 (GLP-2), PGDPs with intestinotrophic activity [8,9]. Notably, circulating levels of endogenous GLP-2 rise rapidly following gut injury or resection [10,11], suggesting that enteroendocrine L cells function as a sensor for mucosal integrity. Exogenous GLP-2 administration robustly stimulates crypt cell proliferation, leading to sustained expansion of the mucosal small bowel epithelium and enhanced capacity for nutrient absorption [9,12]. The proliferative and pro-absorptive actions of GLP-2 are sustained in preclinical animal models of short bowel syndrome [10,13], fostering development of a degradation- and DPP-4-resistant GLP-2 analogue, teduglutide [14], for the treatment of human subjects with parenteral nutrition-dependent short bowel syndrome [15,16].

Although chronic administration of teduglutide enhances the capacity for nutrient absorption in both adults and children with intestinal failure [17,18], the mechanisms through which activation of GLP-2 receptor (GLP-2R) signaling rapidly promotes uptake of digested carbohydrates, fats, and proteins, are poorly understood [19]. Here we examined whether and how acute GLP-2 signaling augments intestinal amino acid (AA) absorption in mice. We identified candidate AA transporters transducing GLP-2 action and demonstrate that loss of GLP-2R signaling in *Glp2r*$^{-/-}$ mice leads to reduced AA absorption. We show that GLP-2 robustly activates the mTORC1 pathway in the murine small intestine. Collectively, these findings demonstrate that GLP-2 controls energy and AA absorption through pathways engaging AA uptake, linking L cell GLP-2 to physiological mechanisms controlling intestinal AA sensing and absorption *in vivo*.

2. MATERIALS AND METHODS

2.1. Source of animals

Colony generation, breeding, and genotyping strategies of *Glp2r*$^{-/-}$ and *Glp1r*$^{-/-}$ mice on the C57BL/6 background have been reported [20–22]. Wild-type *Glp2r*$^{+/+}$ and *Glp1r*$^{+/+}$ littermate mice were used as controls for all experiments. Additional wildtype C57BL/6 mice were ordered from The Jackson Laboratory. All experiments were performed in mice aged 10–14 weeks old. Mice were bred and housed at TCP (Toronto Centre of Phenogenomics) with free access to food and water. All animal experiments were approved by the Animal Care Committee of Mount Sinai Hospital, under conditions consistent with ARRIVE guidelines. For all experiments involving fasting, mice were housed in cages lined with a raised metal-grid bottom with free access to water for the duration of the experiments.

2.2. Peptides, drugs and treatments

Stable isotope-labelled AAs for LC-MS/MS *in vivo* experiments were purchased from Cambridge Isotope Laboratories, Inc. (Andover, USA) including: L-Guanido $^{15}N_2$-Arginine:HCl (NLM-395-0), L-^{15}N-Valine (NLM-316-SP), L-1-^{13}C-Methionine (CLM-3267-0), L-^{15}N-Isoleucine (NLM-292-0), L-1-^{13}C-Leucine (CLM-468-0), L-1-^{13}C-Phenylalanine (CLM-762-SP), L-α^{15}N-Lysine:2HCl (NLM-143-0), L-ring-2-^{13}C-Histidine:HCl:H_2O (CLM-1512-0), L-^{15}N-Threonine (NLM-742-SP), L-$^{15}N_2$-ornithine:HCL (NLM-3610-0). Non-labeled amino acids were purchased from Sigma–Aldrich (Oakville, ON). Radiolabeled L-[4,5-^{3}H(N)]-Lysine and D-[1-^{14}C]-Mannitol used for Ussing chamber experiments were from Perkin Elmer (Boston, MA). Human [Gly_2]-GLP-2, herein referred to as GLP-2, was from Pepceutical Ltd (Nottingham, UK), Exendin-4 (Ex-4) was from CHI scientific (Maynard, MA), rapamycin (Rapamune oral solution) was from Wyeth (Montreal, QC), wortmannin, an inhibitor of phosphatidylinositol-3-kinase (PI3K), was from Calbiochem (EMD Chemicals San Diego, CA, Cat# 681675), and tetrodotoxin was from Alomone Labs (Jerusalem, Israel, Cat# T-550). 10% whey protein mix (100% Any Whey Protein, dissolved in water), a liquid mixed meal (Ensure Plus Calories), or olive oil (Cat# 01514) used for gavaging mice (200 μl) were from ON (Sunrise, FL), Abbott Nutrition (Abbott Laboratories Ltd, Saint-Laurent, QC), and Sigma–Aldrich (St Louis, MO), respectively.

2.3. Assessment of intestinal adaptation following refeeding

Mice were either fasted for 24 h or fasted followed by a 24 h refeeding period with free access to food. For rapamycin experiments, the mTORC1 inhibitor was administered orally (2 mg/kg) 30 min prior to the 24 h refeeding period. At the end of the fasting or refeeding period, mice were sacrificed by CO_2 inhalation, and the entire small intestine from the stomach to the cecum was removed. Small bowel length was measured under tension by suspending a 1-g weight from the distal end, prior to flushing with PBS to remove luminal content. The entire small bowel was then blotted to remove free liquid before being weighed.

2.4. Assessment of gastric emptying

The acetaminophen absorption test was used to assess the rate of gastric emptying. After an overnight fast, mice were gavaged with a solution that contained 1% (w/v) acetaminophen (Sigma–Aldrich) in water. The dose of acetaminophen administered was 100 mg/kg. Tail vein blood (50 μL) was collected into heparin-coated tubes at 0, 15, 30, and 60 min after acetaminophen administration. Plasma was separated by centrifugation at 4 °C and stored at −80 °C until measurement of acetaminophen levels using an enzymatic-spectrophotometric assay (Sekisui Diagnostics, Charlottetown, PE).

2.5. LC-MS/MS analysis of stable AA isotopes

Following fasting (as indicated in the figure legends), mice were given an oral gavage of a stable isotope-labeled essential AA cocktail. Tail vein blood was collected and 25 μL plasma was derivatized for LC-MS/MS HPLC analysis. 500 μL methanol was added to plasma and centrifuged at 13,000 rpm for 20 min. Supernatant was transferred to derivatizing tubes and dried under nitrogen. Samples were butylated with 3N HCl-butanol at 65 °C for 20 min and re-dried under nitrogen before reconstitution in 100 μL 50% Acetonitrile/0.1% formic acid buffer. Samples were run in 25% Acetonitrile at 1 mL/min and

analyzed an API 4000 triple quadrupole mass spectrometer (Applied Biosystems-MDS Sciex) in a positive electrospray ionization mode. This was coupled to an Aligent 1100 HPLC system (Aligent Technologies Canada Inc). All aspects of the system operation and data acquisition were controlled with Analyst NT software (version 1.4.1; Applied Biosystems) by the Analytical Facility for Bioactive Molecules (AFBM), The Hospital for Sick Children, Toronto, Canada.

2.6. Gene expression analysis

Total RNA from full thickness jejunal tissue was extracted by the guanidinium thiocyanate method, and cDNA synthesis performed by random hexamers and SuperScript III (Invitrogen). Real-time quantitative PCR was performed on an ABI Prism 7900HT Sequence Detection System (Applied Biosystems, Foster City, CA) with TaqMan Universal PCR Master Mix and TaqMan Gene Expression Assays (Applied Biosystems) for the following genes: *cyclophilin* (PPia: Mm02342430_g1), *slc7a9* ($b^{0,+}$AT: Mm00445269_m1), *slc3a1* (rBAT: Mm00486218_m1), *slc3a2* (4F2hc: Mm00500521), *slc7a1* (CAT-1: Mm01219060_m1), *slc7a5* (LAT1: Mm00441516_m1), *slc7a8* (LAT2: Mm01318974_m1), *slc7a7* (y + LAT1: Mm00448764_m1), *slc7a6* (y + LAT2: Mm00626779_m1), *slc6a19* (B0 AT1: Mm01352157_m1), *Ace2* (Mm01159003_m1), *slc1a5* (Asct2: Mm00436603_m1). Relative quantification of transcript levels was analyzed using the $2^{-\Delta C_t}$ method with C_t values obtained from PCR amplification kinetics measured by the ABI PRISM SDS 2.1 software. Cyclophilin RNA (*Ppia*) was used for normalization as its intestinal expression remained unaltered independent of mouse genotype or treatment.

2.7. Intestinal tissue preparation and brush border membrane vesicle (BBMV) isolation for protein expression analysis

2.7.1. Mucosal scrapings

2 cm segments from the proximal jejunum were collected and flash frozen at −80 °C. Tissues were thawed on a cold metal plate (embedded with ice) and cut longitudinally, mucosal side facing up. One glass slide was anchored to one end of the tissue while the other glass slide (at 45°), with mild pressure, scraped the mucosa from the serosal muscle layer. Scrapings were immediately transferred to 1.5 mL Eppendorf tubes for protein extraction.

2.7.2. Protein extraction

Tissue extracts were prepared by homogenization of jejunal segments (2 cm), or mucosal scrapings, in ice-cold RIPA buffer (1% Nonidet P-40, 0.5% sodium deoxycholate, and 0.1% sodium dodecyl sulfate in Tris-buffered saline) supplemented with protease and phosphatase inhibitors (Sigma–Aldrich), 5 mmol/L sodium flouride, 5 mmol/L β-glycerophosphate, and 200 μmol/L sodium orthovanadate and centrifuged at 10,000 g for 20 min. Supernatant was collected and stored at −80 °C.

2.7.3. Brush border membrane vesicles (BBMV)

Mucosal scrapings were collected from the entire gut and transferred to 15 mL cold homogenization buffer (300 mM D-mannitol, 5 mM EGTA, 12 mM Tris-base, pH 7.1) supplemented with complete protease inhibitor tablets (Sigma–Aldrich, Oakville, ON). Following 3 min homogenization, 20 mL cold water and 12 mM $MgCl_2$ were added to each sample for BBMV divalent cation precipitation and mixed by inversion. Samples were centrifuged at 4,500 rpm at 4 °C for 15 min to remove aggregated membranes and supernatant decanted for second centrifugation at 16,000 rpm at 4 °C for 30 min. Pellets were re-suspended in 150 mM D-mannitol, 2.5 mM EGTA, 6 mM Tris–HCl, pH 7.1, precipitated a second time with 12 mM $MgCl_2$ on ice for 15 min, then centrifuged again at 16,000 rpm at 4 °C for 30 min. The final BBMV pellet was re-suspended in sterile PBS and stored at −80 °C.

2.8. Western blotting

Samples for isolated BBMVs (25 μg), full thickness jejunal segments (45 μg), or mucosal scrapings (50 μg) were separated by SDS-PAGE and blotted onto nitrocellulose membranes. After blocking non-specific binding sites, membranes for BBMVs were probed for 4F2hc (Cat# sc-7094), PepT1 (Cat# sc-20653), β-actin (Cat# sc-130656) from Santa Cruz Biotechnology Inc. (Dallas, TX), B^0 AT1 (a kind gift from Stephan Broer, Australian National University, Canberra, Australia [23]) and Ace2 (Cat# ab87436, Abcam Inc, Toronto, ON), whereas jejunal segments were probed for p-S6 (Ser-235/236, Cat# D68F8), S6 (Cat#2217), p-Akt (Ser-473 Cat#9271), Akt (Cat#9272 Cell Signaling Technology, Danvers, MA), 4E-BP1 (Cat#A300-501A, Bethyl Laboratories Inc., Montgomery, Tx), and Hsp90 (Cat #610418, BD Transduction Laboratories, BD Biosciences, San Jose, CA) using recommended antibody dilutions and detected by enhanced chemiluminescence using Supersignal West Pico Chemiluminescent Substrate (Cat#34080, Thermo Scientific, Rockford, IL). Images were taken using a Kodak Image Station 4000 mm Pro and signal intensity was quantified using Carestream Molecular Imaging Software, Standard Edition V.5.0.2.30 (Carestream Health Inc., Vaughan, ON) or by Scion image (NIH).

2.9. Assessment of AA transport in small intestine *ex vivo*

Vectorial lysine transport was determined in mouse jejunal tissue preparations mounted into Ussing chambers (Physiologic Instruments, San Diego, CA), bathed in Kreb's buffer and gassed with 95% O_2-5% CO_2 as previously described [21]. A 0.3 cm^2 aperture slider was used for full thickness preparations, whereas the aperture was 0.03 cm^2 when seromuscular-stripped tissue preparations were utilized. Following a 20 min tissue equilibration period (time 0), 20 mM cold lysine, 20 μCi ^{3}H-lysine and 1 μCi ^{14}C-mannitol was added to the mucosal chamber, while 20 mM of glucose and mannitol each were added to the serosal chamber. GLP-2 (200 nM) was added to the serosal chamber at time 0 min; drugs [rapamycin (10^{-7} M), wortmannin (10^{-7} M), or tetrodotoxin (2 μM)] were added to the serosal chamber at time 40 min. Samples were collected from the serosal chamber at regular intervals and radioactivity was measured using the Beckman Coulter LS 6500 Multi-purpose scintillation counter. The paracellular permeability marker mannitol was used as in indicator of the integrity of the intestinal tissue preparations.

2.10. Statistics

Data are represented as means ± SEM. All data were analyzed by t-test, one-way ANOVA, or two-way ANOVA where appropriate using GraphPad Prism v5.0 (GraphPad Software, San Diego, California) and Statistica v6.0 (StatSoft, Inc. Tulsa, OK).

3. RESULTS

3.1. GLP-2, but not GLP-1, activates mTORC1 in a rapamycin-sensitive manner

As GLP-2 augments nutrient absorption and mechanistic target of rapamycin (mTOR) is a key sensor of nutritional status [24], we examined whether GLP-2 promotes activation of the mTOR signaling pathway in the intestine. GLP-2, but not the GLP-1 receptor agonist

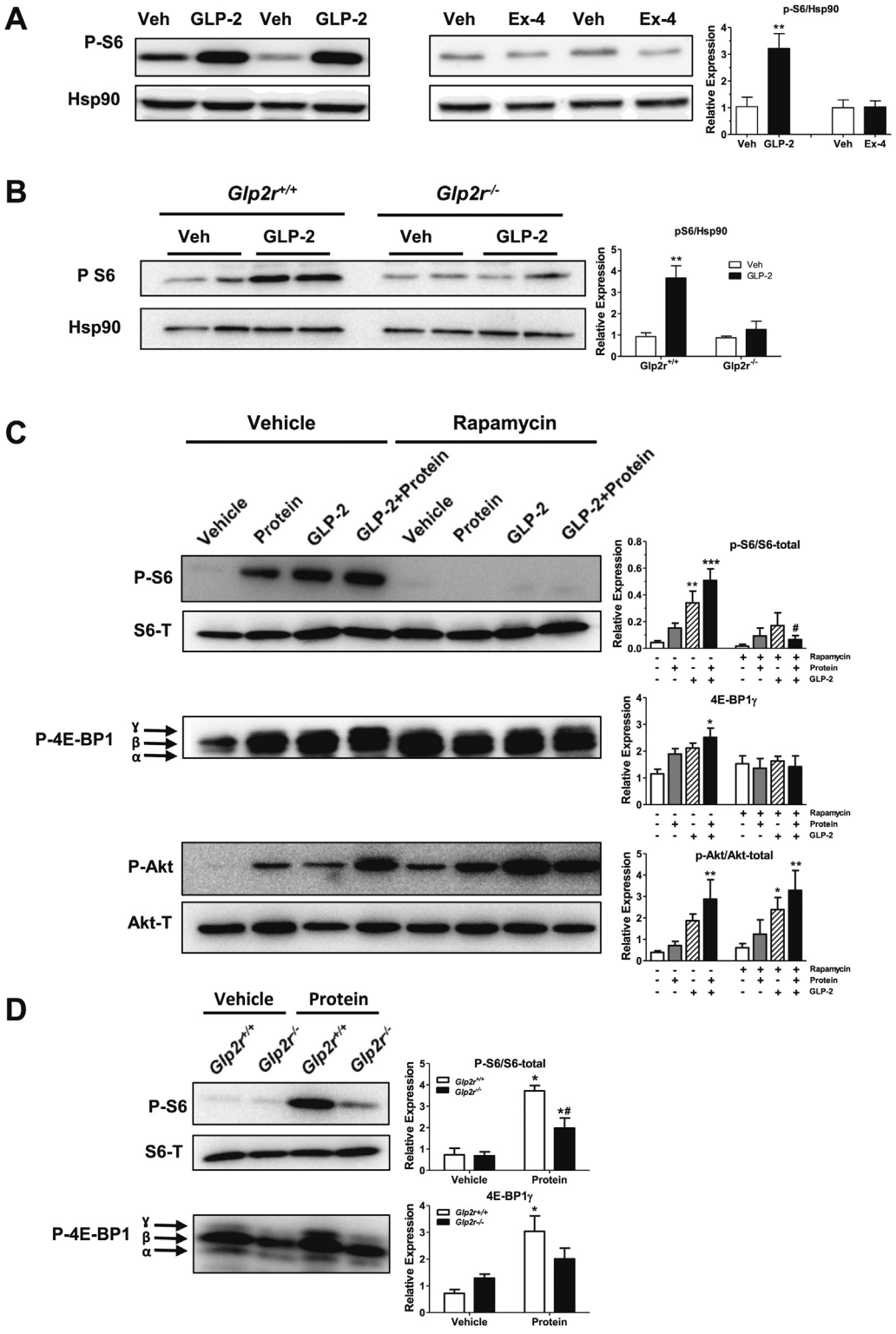

Figure 1: GLP-2 activates mTORC1 in a rapamycin-sensitive manner. (A and B) Representative Western blot analysis of phosphorylated S6 and Hsp90 (loading control) in full thickness jejunal segments from overnight fasted C57BL/6J mice injected intraperitoneally (i.p.) with vehicle (PBS), GLP-2 (53 nmol/kg = 200 μg/kg), or Ex-4 (10 nmol/kg) (A), or overnight fasted *Glp2r*$^{+/+}$ and *Glp2r*$^{-/-}$ mice injected (i.p.) with vehicle (PBS), or GLP-2 (200 μg/kg) (B) for 1 h. Bar diagrams represent phospho-S6 levels normalized to Hsp90. Data are mean ± SEM. For panel (A) n = 4 mice per group from 2 independent experiments. For panel (B) n = 2–3 mice per group from 2 independent experiments. **p < 0.01 vehicle *vs.* treatment. (C) Western blot analysis of phosphorylated S6, Akt, or 4E-BP1 in jejunal mucosal scrapings of overnight fasted C57BL/6J mice treated with oral rapamycin (2 mg/kg) or vehicle. 30 min after rapamycin, mice were injected (i.p.) with vehicle or GLP-2 (200 μg/kg), followed by an oral gavage of a 10% protein mix 30 min later. Mice were sacrificed 30 min after the protein gavage. Bar diagrams represent phospho-protein expression normalized to paired total protein levels, or the intensity of the hyperphosphorylated γ-isoform band of 4E-BP1. Data are mean ± SEM, n = 3–5 mice per group. *p < 0.05, **p < 0.01, ***p < 0.001 vehicle *vs.* treatment. #p < 0.05 vehicle-treatment *vs.* rapamycin-treatment. (D) Following an overnight fast, *Glp2r*$^{+/+}$ or *Glp2r*$^{-/-}$ mice were orally gavaged with a 10% protein mix 30 min prior to collection of

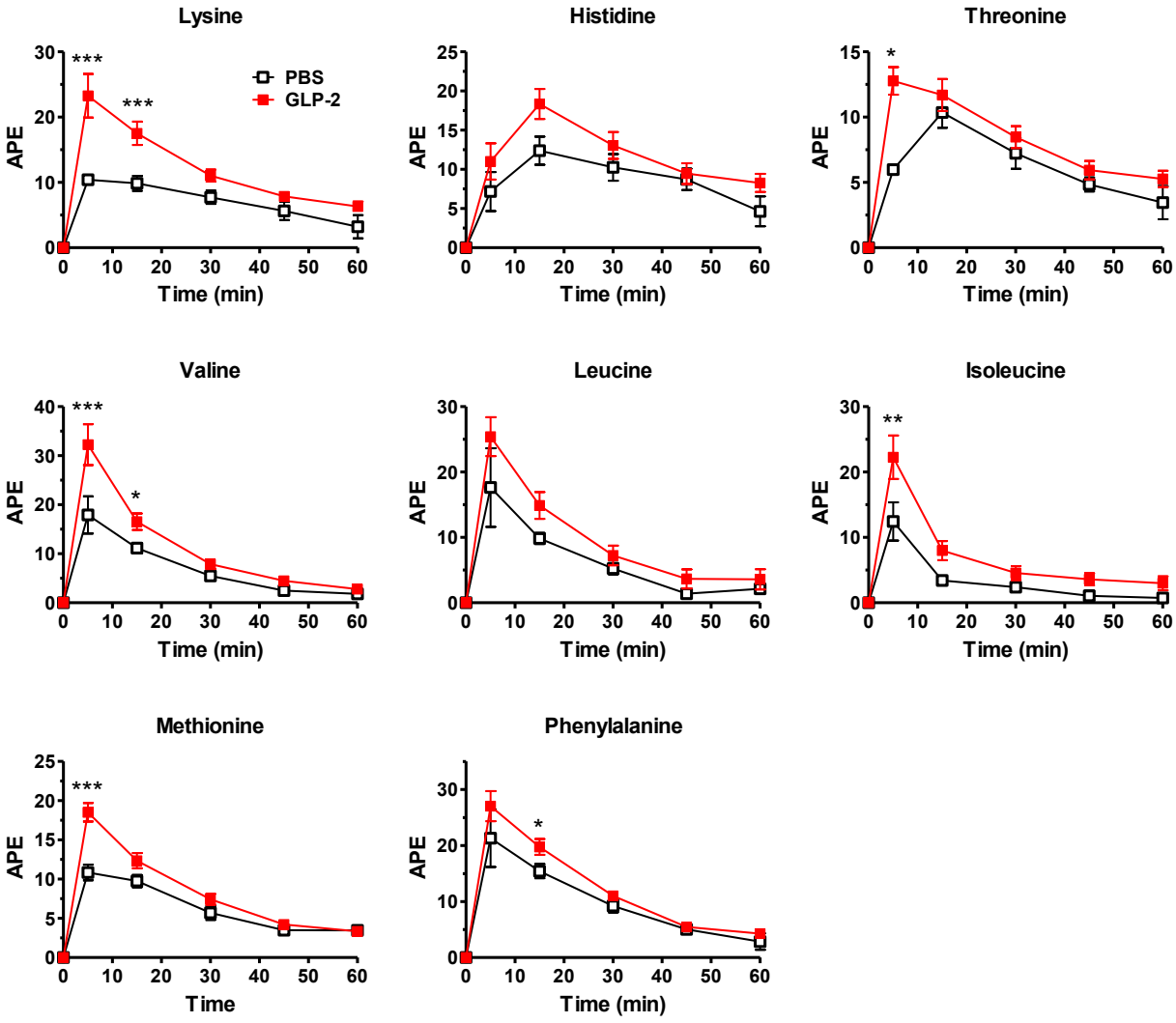

Figure 2: GLP-2 treatment enhances AA absorption *in vivo*. C57BL/6J mice were fasted for 5 h, GLP-2 (100 μg/kg) or vehicle was then administered (i.p.) 10 min prior to an oral gavage of a stable isotope-labeled essential AA cocktail. Tail vein blood was collected at 5 min and every 15 min up to 1 h. Plasma samples were derivatized and analyzed by LC-MS/MS HPLC. Data are mean ± SEM, n = 7–12 from 2 independent experiments. APE, atom percent over excess. *p < 0.05, **p < 0.01, ***p < 0.001 vehicle *vs.* GLP-2 treatment.

exendin-4 (Ex-4), acutely induced S6 ribosomal protein phosphorylation in the jejunum of WT mice (Figure 1A). Moreover, activation of this pathway was dependent on the canonical GLP-2 receptor, as GLP-2 failed to induce S6 phosphorylation in the intestine of *Glp2r*$^{-/-}$ mice (Figure 1B). Pretreatment with rapamycin (an inhibitor of mTOR complex 1 (mTORC1)) abolished S6 phosphorylation in response to exogenous GLP-2 (Figure 1C). Moreover, jejunal S6 phosphorylation was also rapidly increased following oral gavage of a 10% protein mixture and similarly extinguished by rapamycin (Figure 1C). Phosphorylation of eukaryotic translation initiation factor 4E (eIF4e)-binding protein 1 (4E-BP1), another downstream effector protein of the mTORC1 pathway whose activation is required for protein translation [25], also increased in response to GLP-2 or following oral protein administration, principally indicated by the increase in the hyperphosphorylated γ-isoform band (Figure 1C). Notably, combined administration of oral protein and parenteral GLP-2 administration further augmented the extent of both S6 and 4E-BP1 phosphorylation. Similarly, jejunal Akt phosphorylation was increased in response to either GLP-2 or oral protein and further augmented by combination treatment. In contrast to findings with S6 and 4E-BP1, rapamycin pretreatment did not affect Akt activation by either GLP-2 or protein gavage, consistent with Akt lying upstream of mTORC1 activation [25] (Figure 1C).

Fasting induces intestinal atrophy and re-feeding restores gut mucosal mass in part through a GLP-2R-dependent pathway [20,26]. In accordance with mTORC1 functioning as key sensor of nutrient availability, rapamycin pretreatment prevented refeeding-induced small intestinal mucosal adaptation (Supplementary Figure 1A). Furthermore, whereas *Glp2r*$^{-/-}$ mice exhibit an impaired refeeding-induced small intestinal adaptation [20], fasting-induced small

mucosal scrapings from jejunum to measure phosphorylation of S6 and 4E-BP1 by immunoblotting. Bar diagrams represent phospho-S6 expression normalized to total S6 protein levels, or the intensity of the hyperphosphorylated γ-isoform band of 4E-BP1. Data are mean ± SEM, n = 4 mice per group. *p < 0.05 vehicle *vs.* protein gavage, #p < 0.05 *Glp2r*$^{+/+}$ *vs.* *Glp2r*$^{-/-}$ mice.

intestinal hypoplasia was fully reversed following refeeding in *Glp1r*$^{-/-}$ mice (Supplementary Figure 1B). Thus, although GLP-1 and GLP-2 are co-secreted upon nutrient ingestion, only GLP-2 activates mTORC1-associated nutrient sensing pathways linked to GLP-2R-dependent signals required for intestinal adaptation following refeeding.

3.2. Activation of mTORC1 effector substrates in response to protein is attenuated in *Glp2r*$^{-/-}$ mice

To determine whether GLP-2R-dependent signals are essential for mTORC1 activation in response to nutrients, phosphorylation levels of mTORC1 effector proteins were measured in overnight-fasted *Glp2r*$^{+/+}$ and *Glp2r*$^{-/-}$ mice acutely challenged with an oral gavage of lipid (olive oil), Ensure (a liquid meal replacement), or protein (10% whey protein mixture). Under fasted conditions, basal levels of phosphorylated 4E-BP1 and S6 were comparable between *Glp2r*$^{+/+}$ and *Glp2r*$^{-/-}$ mice (Figure 1D, Supplementary Figure 1C). Likewise, S6 phosphorylation levels were similar in jejunal extracts from *Glp2r*$^{+/+}$ and *Glp2r*$^{-/-}$ mice following an oral gavage of Ensure (Supplementary Figure 1C). In contrast, the phosphorylation of 4E-BP1 (as indicated by the γ-isoform) and S6 were significantly increased in *Glp2r*$^{+/+}$ mice, but blunted in *Glp2r*$^{-/-}$ mice following an oral protein load (Figure 1D, Supplementary Figure 1C). S6 phosphorylation levels induced by lipid also trended lower in *Glp2r*$^{-/-}$ (Supplementary Figure 1C). Thus, mTORC1-dependent jejunal protein sensing is impaired in the absence of a functional GLP-2R.

3.3. Amino acid transport is regulated by GLP-2

As amino acids are strong activators of the mTOR pathway [27] and mTORC1 activation in response to protein was reduced in *Glp2r*$^{-/-}$ mice, we examined the importance of GLP-2 for intestinal AA absorption. Acute administration of GLP-2 to fasted mice increased levels of plasma lysine and multiple essential amino acids (EAAs) following enteral gavage of a stable isotope-labeled AA cocktail, compared to levels detected in vehicle-treated mice (Figure 2). Furthermore, plasma AAs were significantly reduced following AA gavage in *Glp2r*$^{-/-}$ mice compared to *Glp2r*$^{+/+}$ littermates (Figure 3). To rule out the possibility that differences in plasma AA levels reflected reduced gastric motility, we assessed gastric emptying, which was not different between *Glp2r*$^{+/+}$ and *Glp2r*$^{-/-}$ mice (Supplementary Figure 2A). Similarly, AA clearance rate, approximated by measuring changes in AA levels after intravenous administration, was not different between *Glp2r*$^{+/+}$ and *Glp2r*$^{-/-}$ mice (Supplementary Figure 2B). Taken together, these gain- and loss-of-function studies reveal that GLP-2 stimulates intestinal AA transport and the mTOR signaling pathway, whereas gut AA transport is impaired in *Glp2r*$^{-/-}$ mice.

3.4. Intestinal mRNA transcripts for $b^{0,+}$AT and LAT1 are reduced in refed *Glp2r*$^{-/-}$ mice

As GLP-2 upregulates transport of multiple AAs, we measured intestinal levels of mRNA transcripts encoding AA transporters involved in uptake and absorption of essential AAs under fasted and fed states, in both *Glp2r*$^{-/-}$ and littermate control *Glp2*$^{+/+}$ mice. As shown in Supplementary Figure 3, under fasting conditions, no differences were observed in transcript levels for: i) system $b^{0,+}$ ($b^{0,+}$AT and rBAT), which mediates apical uptake of cationic AA and cysteine in exchange for intracellular neutral AA; ii) system B^0 (B^0AT1), which mediates apical uptake of all neutral AA; iii) angiotensin converting enzyme 2 (Ace2), which is required for B^0AT1 localization to the brush-border membrane; iv) Asct2, an apical transporter for small neutral AA and anionic AA; v) system L (4F2hc and LAT1 or LAT2), which releases smaller intracellular neutral AA basolaterally in exchange for larger extracellular neutral AA; vi) system y^+L (4F2hc and y^+LAT1 or y^+LAT2), which releases intracellular cationic AA basolaterally in exchange for extracellular neutral AA together with Na^{2+}; or vii) system y^+ (CAT-1), involved in basolateral transport of cationic amino acids. In contrast, mRNA levels for the light-chain subunit $b^{0,+}$AT (*slc7a9*) of the

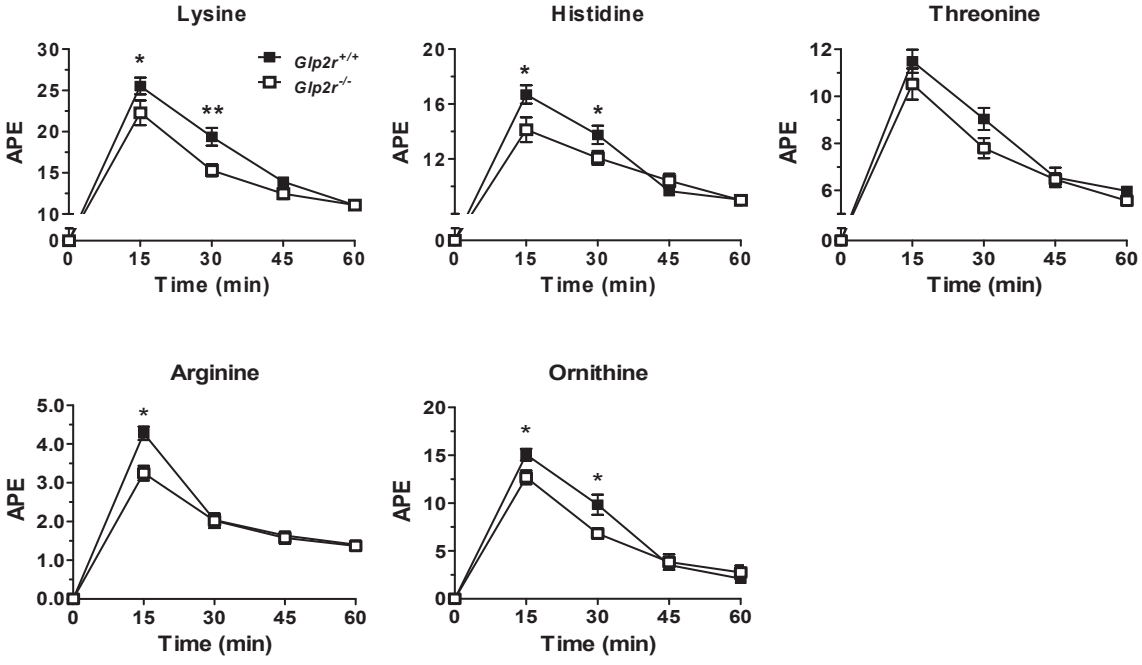

Figure 3: AA absorption is reduced in *Glp2r*$^{-/-}$ mice *in vivo*. Male *Glp2r*$^{-/-}$ and *Glp2r*$^{+/+}$ littermate mice were fasted overnight and gavaged with a cocktail of stable isotope-labeled AAs. Tail vein blood was collected every 15 min up to 1hr and plasma was processed and derivatized for LC-MS/MS HPLC. APE, atoms per excess. Data are mean ± SEM. n = 6–8 per group. *p < 0.05, **p < 0.01 *Glp2r*$^{+/+}$ *vs.* *Glp2r*$^{-/-}$ mice.

cationic AA transporter significantly increased in *Glp2*$^{+/+}$, but not in refed *Glp2r*$^{-/-}$ mice (Supplementary Figure 3). Levels of *slc7a9* were also reduced in the small bowel of *ad libitum* fed *Glp2r*$^{-/-}$ mice (data not shown). Transcript levels for LAT1 (*slc7a5*) were also significantly lower in refed *Glp2r*$^{-/-}$ mice compared to *Glp2r*$^{+/+}$ littermate controls (Supplementary Figure 3).

3.5. Expression of intestinal amino acid transporters in response to re-feeding

As the diminished AA absorption and reduced intestinal mTORC1 activation in *Glp2r*$^{-/-}$ mice in response to protein intake could be due to alterations in protein expression and/or translocation of AA transporters to the plasma membrane, we examined the expression of AA transporters in BBMVs of fasted mice or following an oral protein gavage. Levels of B^0AT1, the major apical neutral AA transporter in the intestine, its ancillary protein Ace2, or the small peptide transporter PepT1 were similar in intestinal BBMVs isolated from fasted *Glp2r*$^{+/+}$ *vs.* *Glp2r*$^{-/-}$ mice and 30 min following an oral protein load (Figure 4A and B). In contrast, the heavy-chain subunit 4F2hc was significantly increased in these membrane preparations in *Glp2r*$^{+/+}$ mice following an acute oral protein challenge, whereas this increase was attenuated in *Glp2r*$^{-/-}$ mice (Figure 4C). Thus, altered mRNA expression of the light-chain subunit ($b^{0,+}$AT) that participates in dibasic AA transport, and membrane-associated protein expression of the heavy chain subunit (4F2hc) responsible for dibasic and neutral AA transport, may contribute to the impaired AA absorption observed in *Glp2r*$^{-/-}$ mice.

3.6. GLP-2-stimulates lysine transport independently of blood flow

As GLP-2 is known to increase intestinal blood flow [28], which may indirectly contribute to augmentation of AA absorption observed *in vivo*, we examined AA transport *ex vivo* in jejunal tissue preparations mounted in an Ussing chamber. Lysine mucosal to serosal transport was increased in full thickness jejunal preparations from wild-type mice pretreated with GLP-2 *in vivo* (Figure 5A). Moreover, lysine transport also increased within minutes when seromuscular-stripped jejunal tissue preparations were challenged with GLP-2 added to the serosal compartment of the Ussing chamber (Figure 5B). In contrast, basal lysine transport was markedly attenuated in isolated jejunal strips from *Glp2r*$^{-/-}$ mice *ex vivo* compared to *Glp2r*$^{+/+}$ mice (Figure 5C). GLP-2-stimulated lysine transport in seromuscular-stripped jejunal preparations from wild-type mice was significantly reduced following *ex vivo* administration of inhibitors for PI3K (wortmannin), mTOR (rapamycin), or neuronal activity (tetrodotoxin) (Figure 5D–F). Hence, GLP-2 directly stimulated lysine uptake in the small intestine independently of blood flow, through mechanisms requiring neuronal transmission as well as the Akt-mTOR signaling pathway.

4. DISCUSSION

Enteroendocrine L cells have assumed increasing importance in the physiology of energy homeostasis, acting as an endocrine hub coordinating the ingestion, absorption, and disposal of available nutrients. GLP-1, the prototype and best studied L cell-derived PGDP, acts both proximally, to control the rate of passage of digested nutrients along the gut and expand mucosal surface area, and more distally beyond the gut mucosa, to facilitate the uptake of nutrients by regulating a brain-pancreatic islet axis to ensure that meal-related nutrient influx is balanced by physiological control of islet hormone secretion and energy assimilation. These properties of GLP-1, taken together with its favorable cardiometabolic actions, have fostered great interest in

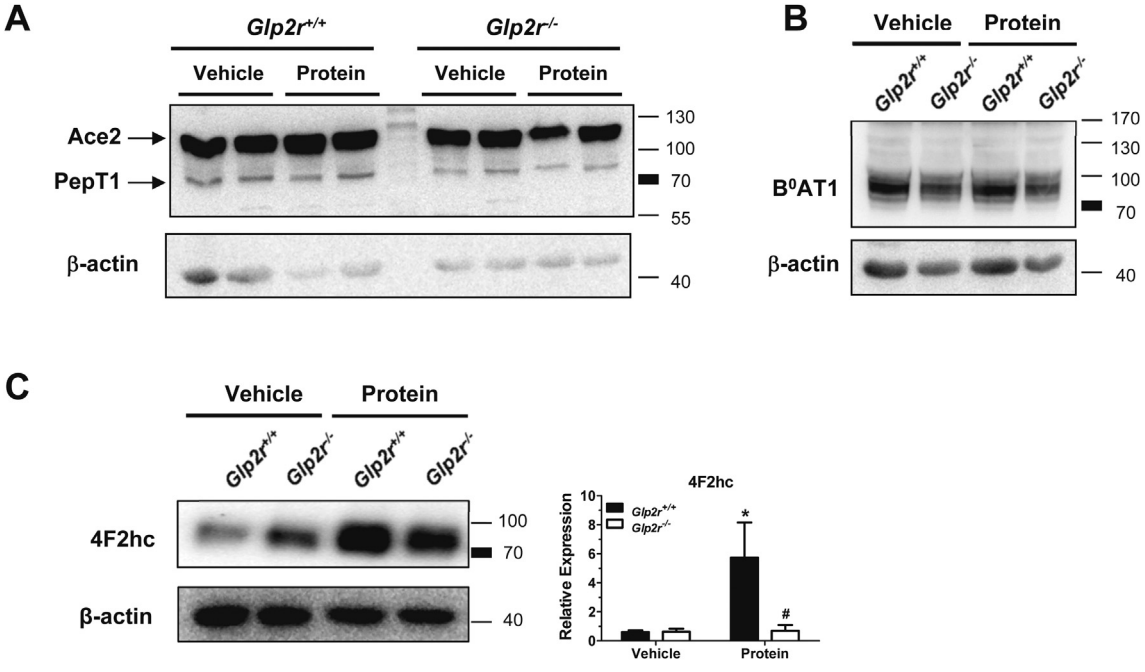

Figure 4: Impaired membrane translocation of the heavy chain dibasic transporter 4F2hc in response to protein feeding in *Glp2r*$^{-/-}$ mice. Overnight fasted *Glp2r*$^{-/-}$ and *Glp2r*$^{+/+}$ littermate mice were orally gavaged with either vehicle or 10% protein mix 30 min prior to small intestinal BBMV isolation. Membrane preparations were immunoblotted for (A) Ace2 and PepT1, (B) B^0AT1, (C) the heavy chain dibasic transporter 4F2hc, or β-actin as a loading control. Representative immunoblots are shown of 2–3 mice per group from 2 independent experiments. In panel (C) Bar diagram represent 4F2hc protein levels normalized to β-actin. Data are mean ± SEM, n = 3 per group. *p < 0.05 vehicle *vs.* protein, #p < 0.05 *Glp2r*$^{+/+}$ *vs.* *Glp2r*$^{-/-}$ mice.

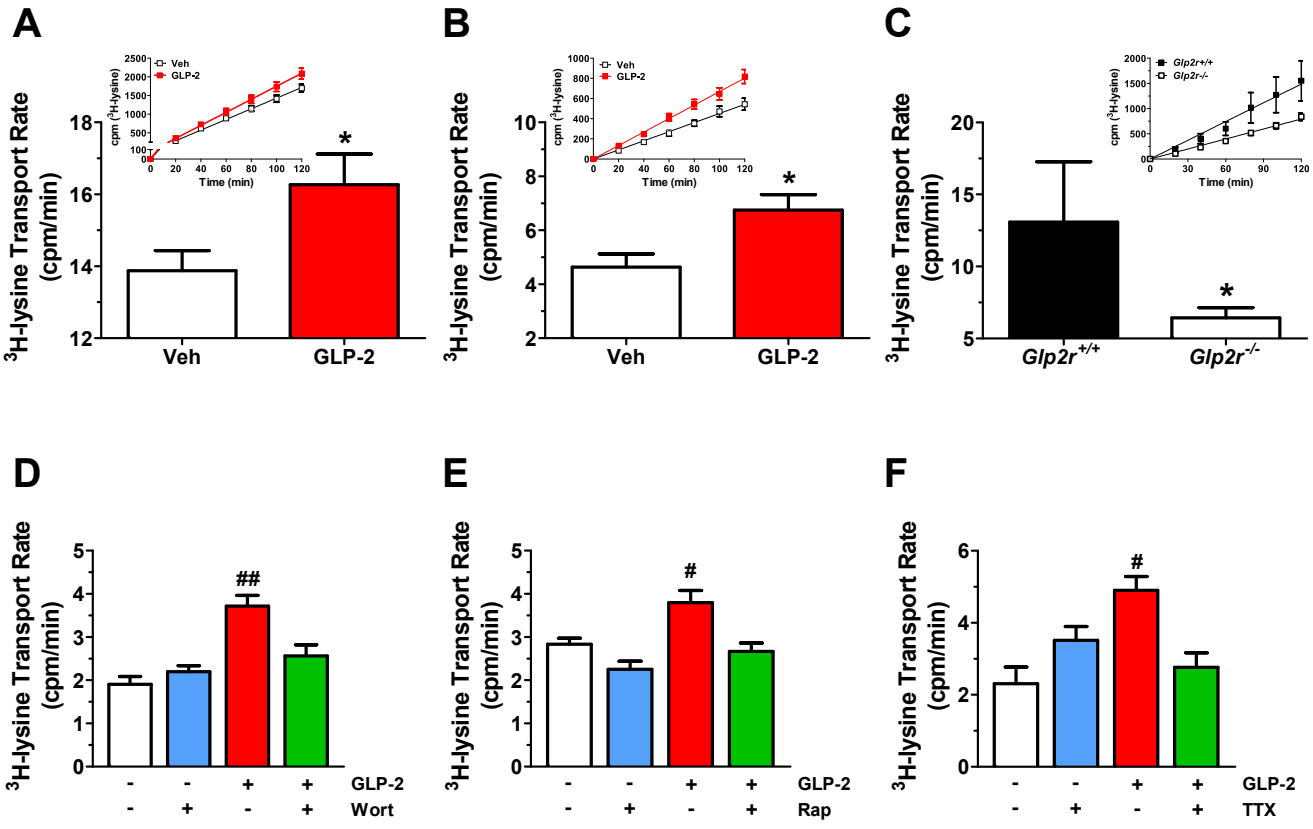

Figure 5: GLP-2 stimulates lysine transport in murine small intestine independently of blood flow but requires PI3K-AKT/mTORC1 signaling and enteric neuronal activity. (A) C57BL/6J mice were treated acutely *in vivo* with either vehicle or GLP-2 (100 μg/kg) 30 min prior to tissue collection. ^{3}H-Lysine transport was measured in full thickness jejunal tissue preparations mounted into Ussing chambers as described in Section 2. Data are mean ± SEM, n = 6–8 independent experiments performed in triplicate. *p < 0.05 GLP-2 *vs.* vehicle. (B) Seromuscular-stripped jejunal sections from C57BL/6J mice were mounted into Ussing chambers to measure ^{3}H-Lysine transport rate following serosal addition of vehicle or GLP-2 (200 nM). Data are mean ± SEM, n = 7 independent experiments performed in triplicate. *p < 0.05 GLP-2 *vs.* vehicle. (C) ^{3}H-Lysine transport using full thickness jejunal sections from *Glp2r*$^{-/-}$ mice and *Glp2r*$^{+/+}$ littermate controls. Data are mean ± SEM, n = 4–6 independent experiments performed in triplicate. *p < 0.05 *Glp2r*$^{+/+}$ *vs.* *Glp2r*$^{-/-}$ mice. For (A–C), insets illustrate representative time-courses of ^{3}H-Lysine appearance in the serosal chamber which were used to determine transport rate. Transport rate is operationally defined by the slope of the corresponding time course. (D–F) The rate of lysine transport was first assessed in seromuscular-stripped jejunal sections from C57BL/6J mice following the addition of vehicle or GLP-2 (200 nM) to the serosal compartment. 40 min later, either vehicle or (D) Wortmannin (Wort, 10^{-7} M), (E) Rapamycin (Rap, 10^{-7} M), or (F) tetrodotoxin (TTX, 2 μM) was added to the same compartment and lysine transport was re-assessed from 40 to 90 min. Basal and GLP-2-stimulated lysine transport was measured from 0 to 40 min, whereas transport in the presence of the indicated inhibitors was measured from 40 to 90 min #p < 0.05, ##p < 0.01 GLP-2 *vs.* vehicle, or Inhibitor *vs.* GLP-2 + Inhibitor. Data are mean ± SEM, n = 5–6 (D), n = 7–9 (E), or n = 3–6 (F) independent experiments performed in triplicate.

developing new agents that enhance GLP-1 secretion or action for the treatment of metabolic disorders.

Although less well studied, GLP-2 is co-secreted together with GLP-1 from L cells and exerts a number of complementary actions to enable optimal absorption of digested nutrients, including control of intestinal motility, barrier integrity, blood flow, and expansion of mucosal surface area [19]. Here we further distinguish the actions of GLP-1 from those of GLP-2 by demonstrating that GLP-2 controls intestinal AA absorption in an mTORC1-dependent manner. Importantly, our data using isolated intestinal segments *ex vivo* shows that GLP-2 maintains its ability to augment AA transport independent of blood flow, suggesting that GLP-2 acts directly on the intestine to stimulate AA absorption. Notably, we also demonstrate that GLP-2 directly activates mTORC1 signaling. Previous studies have demonstrated that GLP-2 stimulates gut mucosal growth in the setting of enteral nutrient deprivation in part through suppression of proteolysis, leading to preservation of energy availability, and both protein and DNA accretion within the intestinal mucosa [29]. Moreover, GLP-2 rapidly increases blood flow to the proximal small bowel in piglets maintained on parenteral nutrition, findings associated with increased splanchnic glucose uptake, whereas infusion of L-NAME to block the increased blood flow also attenuated changes in glucose uptake [28,30]. Our current findings in mice (not maintained on parenteral nutrition) dissociate changes in blood flow from actions of GLP-2 that acutely increase AA transport. Moreover, *Glp2r*$^{-/-}$ mice exhibit defective absorption of multiple AAs under basal conditions, and isolated jejunal segments from *Glp2r*$^{-/-}$ mice exhibit markedly impaired lysine transport *ex vivo*. Hence, induction of blood flow, while potentially important under defined experimental circumstances, is not essential for mechanisms linking GLP-2R signaling to control of intestinal AA transport.

Although the GLP-2R is not expressed in enterocytes, GLP-2 receptor localization has been challenging, in part due to use of non-specific antisera, limiting interpretation of some of the published literature [19]. Nevertheless, *Glp2r* RNA transcripts have been consistently detected in subpopulations of enteric neurons throughout the small and large intestine [31,32], consistent with an indirect mechanism linking GLP-2-dependent neuronal transmission to control of enterocyte nutrient sensing and absorption. Here we demonstrate that AA

transport is dependent on the ENS, as neuronal inhibition using the voltage-gated sodium channel inhibitor tetrodotoxin prevented GLP-2 stimulated lysine uptake. Enterocytes act as chemoreceptors that inform enteric neurons of available nutrients via neuronal fibers from the submucosal plexus that project and innervate to the mucous layer. The enteric nervous system (ENS) has been implicated in the control of enterocyte renewal [33] and although less information is available regarding ENS signals that direct nutrient uptake from enterocytes, several studies have indicated neural involvement in regulating AA transport activity [34,35]. Our current data is consistent with a model linking EEC-derived GLP-2 to augmentation of enterocyte AA absorption via ENS innervation of the intestinal epithelia.

Amino acids are the basic precursors for protein synthesis and a source of cellular energy but also contribute signals reporting nutrient status and energy availability [36]. Deprivation of AAs, either in the diet of living organisms, or in cell culture media, induces autophagy, highlighting the importance of AA availability in the control of cellular metabolism, cell size, and tissue growth [37,38]. The amino acid response (AAR) pathway is composed of membrane transporters, growth factors, and metabolic enzyme complexes that work in concert to detect and defend against AA deficiency. Indeed, L-glutamine and its membrane transporters are critical for activation of 70 kDa ribosomal protein S6 kinase 1 (S6K1) in the presence of essential AAs, demonstrating that integration of mTORC1-dependent signals that sense AAs begins at the membrane level [38]. Interestingly, B^0AT1-null mice, which lack the main neutral amino acid transporter in both the intestine and kidney, retain AAs in the lumen of the intestine due to incomplete absorption and exhibit enhanced L cell secretory activity, as measured by GLP-1 secretion [39]. Furthermore, several studies have demonstrated that oral administration of certain amino acids, in particular L-glutamine and L-arginine, act as L cell (GLP-1) secretagogues *in vivo* in both rodents [40,41] and in human subjects [42] [43,44]. These same AAs have been shown to play important roles in maintaining gut integrity including preventing intestinal atrophy, improving intestinal barrier function, and reducing inflammation and apoptosis in experimental models of intestinal injury [45]. Since GLP-2 is co-secreted with GLP-1, and many of the previously described actions of GLP-2 overlap with the protective effects induced by enteral AA administration, it seems likely that some of these effects are mediated, at least in part, through luminal AA sensing and secretion of GLP-2 from intestinal L-cells.

The ser/thr protein kinase mTOR is a key sensor of nutritional status, integrating signals from environmental cues with intracellular growth factors and amino acids (AA) to regulate protein synthesis and autophagy. The rapamycin-sensitive mTOR complex 1 (mTORC1) is responsive to AA availability, such that upon activation, phosphorylation of substrates 4E-BP1 and S6K1 promote protein synthesis. Here we demonstrate that basal GLP-2R signaling is essential for control of key components of the intestinal mTOR pathway, as nutrient-stimulated phosphorylation of 4E-BP1 and S6 was significantly reduced in *Glp2r*$^{-/-}$ mice, most likely due to diminished growth factor receptor signaling by known GLP-2R mediators including the ErbB signaling network and insulin-like growth factor-1 (IGF-1) [46,47]. Moreover, *Glp2r*$^{-/-}$ mice exhibit reduced membrane-associated

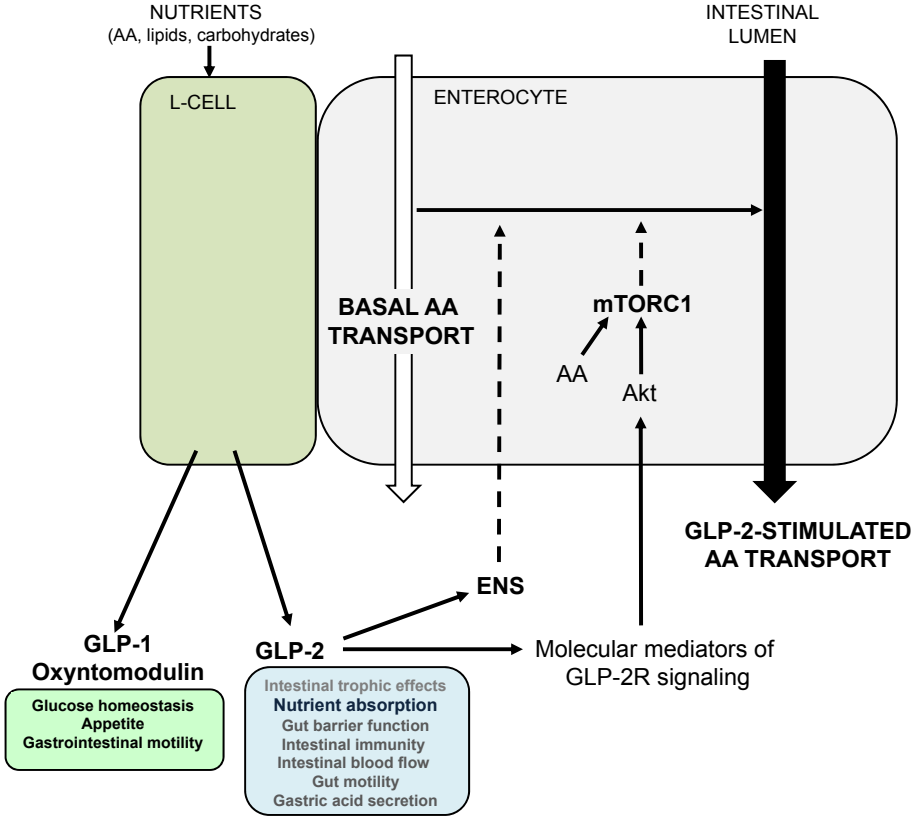

Figure 6: Proposed model by which GLP-2 increases amino acid transport. Nutrient ingestion stimulates GLP-2 release from intestinal L cells. GLP-2R receptor activation on enteric neurons augments amino acid (AA) absorption through a yet unknown mechanism. GLP-2R-dependent signal transduction pathways via known downstream molecular mediators including ErbB ligands and/or insulin-like growth factor-1 (IGF-1) act in concert with AA to stimulate mTORC1 activity in enterocytes. The white arrow represents basal AA absorption, whereas the black arrow represents enhanced AA transport activity. Dashed arrows represent unidentified pathways. ENS: enteric nervous system.

protein levels of 4F2hc following an oral protein challenge. Of direct relevance to GLP-2 action, the glycosylated heavy chain 4F2hc transporter induces system L and y^+L AA transport, mediates transport of essential AAs, and indirectly activates the mTORC1-S6K1 axis. Furthermore, like GLP-2, 4F2hc has also been shown to have proliferative actions on the intestinal epithelium [48]. Hence GLP-2R signaling links jejunal protein sensing to activation of the mTOR pathway, amino acid absorption, and pathways converging on intestinal mucosal growth.

Together, our results identify GLP-2 as a growth factor that also regulates AA transporter expression and directly activates mTORC1 to increase AA absorption in the intestinal epithelium (Figure 6). Our data support a role for a neural signal originating from GLP-2-responsive enteric neurons required for maximal AA transport, but the mediators linking the ENS to enterocyte function remain unknown. AAs are a major contributing source of precursors for fundamental metabolic pathways, including gluconeogenesis, in addition to signaling pathways important for the pathogenesis of metabolic disease and cancer. Our current findings extend GLP-2 action to neuronal innervation, AA transport machinery and mTORC1 signaling, warranting re-evaluation of the role of this classic intestinotrophic hormone in the setting of other metabolic diseases characterized by defective intestinal energy sensing.

Interestingly, both GLP-1 and GLP-2 circulate at markedly increased levels following several types of bariatric surgery [49,50], an intervention associated with rapid weight loss, catabolism, and peripheral muscle protein turnover. Although most studies have focused on the potential role of GLP-1 as a mediator of the changes in body weight and glucose homeostasis arising following bariatric surgery [51], there has been little investigation of whether increased levels of GLP-2 might contribute to metabolic adaptation in these subjects. Notably, plasma AA levels have been noted to increase significantly in the postprandial state after bariatric surgery, whereas basal AA levels have generally remained unchanged, a phenomenon previously attributed to alteration of gastrointestinal motility in these patients [52,53]. Our current findings expand physiological and pharmacological concepts of GLP-2 action beyond the control of gut growth, highlighting the importance of understanding how EEC peptides and their receptors link enteral nutrient sensing to the control of energy availability and nutrient absorption.

ACKNOWLEDGMENTS

This work was support in part by CIHR operating grant 123391, the Canada Research Chairs Program, and the Banting and Best Diabetes Centre-Novo Nordisk Chair in Incretin Biology

CONFLICT OF INTEREST

Daniel Drucker, the University of Toronto, the University Health Network and Shire Pharmaceuticals Inc are partners to a licensing agreement for the clinical development of GLP-2 analogues.

APPENDIX A. SUPPLEMENTARY DATA

Supplementary data related to this article can be found at http://dx.doi.org/10.1016/j.molmet.2017.01.005.

REFERENCES

[1] Psichas, A., Reimann, F., Gribble, F.M., 2015. Gut chemosensing mechanisms. The Journal of Clinical Investigation 125(3):908–917.

[2] Gribble, F.M., Reimann, F., 2016. Enteroendocrine cells: chemosensors in the intestinal epithelium. Annual Review of Physiology 78:277–299.

[3] Drucker, D.J., 2016. Evolving concepts and translational relevance of enteroendocrine cell biology. The Journal of Clinical Endocrinology & Metabolism 101(3):778–786.

[4] Engelstoft, M.S., Egerod, K.L., Lund, M.L., Schwartz, T.W., 2013. Enteroendocrine cell types revisited. Current Opinion in Pharmacology 13(6):912–921.

[5] Sandoval, D.A., D'Alessio, D.A., 2015. Physiology of proglucagon peptides: role of glucagon and GLP-1 in health and disease. Physiological Reviews 95(2):513–548.

[6] Campbell, J.E., Drucker, D.J., 2013. Pharmacology physiology and mechanisms of incretin hormone action. Cell Metabolism 17(4):819–837.

[7] Drucker, D.J., 2015. Deciphering metabolic messages from the gut drives therapeutic innovation: the 2014 banting lecture. Diabetes 64(2):317–326.

[8] Myojo, S., Tsujikawa, T., Sasaki, M., Fujiyama, Y., Bamba, T., 1997. Trophic effects of glicentin on rat small-intestinal mucosa in vivo and in vitro. Journal of Gastroenterology 32(3):300–305.

[9] Drucker, D.J., Ehrlich, P., Asa, S.L., Brubaker, P.L., 1996. Induction of intestinal epithelial proliferation by glucagon-like peptide 2. Proceedings of the National Academy of Sciences United States of America 93:7911–7916.

[10] Ljungmann, K., Hartmann, B., Kissmeyer-Nielsen, P., Flyvbjerg, A., Holst, J.J., Laurberg, S., 2001. Time-dependent intestinal adaptation and GLP-2 alterations after small bowel resection in rats. American Journal of Physiology-Gastrointestinal and Liver Physiology 281(3):G779–G785.

[11] Xiao, Q., Boushey, R.P., Cino, M., Drucker, D.J., Brubaker, P.L., 2000. Circulating levels of glucagon-like peptide-2 in human subjects with inflammatory bowel disease. American Journal of Physiology 278:R1057–R1063.

[12] Brubaker, P.L., Izzo, A., Hill, M., Drucker, D.J., 1997. Intestinal function in mice with small bowel growth induced by glucagon-like peptide-2. American Journal of Physiology 272:E1050–E1058.

[13] Scott, R.B., Kirk, D., MacNaughton, W.K., Meddings, J.B., 1998. GLP-2 augments the adaptive response to massive intestinal resection in rat. American Journal of Physiology 275:G911–G921.

[14] Drucker, D.J., Shi, Q., Crivici, A., Sumner-Smith, M., Tavares, W., Hill, M., et al., 1997. Regulation of the biological activity of glucagon-like peptide 2 in vivo by dipeptidyl peptidase IV. Nature Biotechnology 15(7):673–677.

[15] Jeppesen, P.B., Pertkiewicz, M., Messing, B., Iyer, K., Seidner, D.L., O'Keefe, S.J., et al., 2012. Teduglutide reduces need for parenteral support among patients with short bowel syndrome with intestinal failure. Gastroenterology 143(6):1473–1481.

[16] Tappenden, K.A., Edelman, J., Joelsson, B., 2013. Teduglutide enhances structural adaptation of the small intestinal mucosa in patients with short bowel syndrome. Journal of Clinical Gastroenterology 47(7):602–607.

[17] Jeppesen, P.B., Sanguinetti, E.L., Buchman, A., Howard, L., Scolapio, J.S., Ziegler, T.R., et al., 2005. Teduglutide (ALX-0600), a dipeptidyl peptidase IV resistant glucagon-like peptide 2 analogue, improves intestinal function in short bowel syndrome patients. Gut 54(9):1224–1231.

[18] Carter, B.A., Cohran, V.C., Cole, C.R., Corkins, M.R., Dimmitt, R.A., Duggan, C., et al., 2016. Outcomes from a 12-week, open-label, multicenter clinical trial of teduglutide in pediatric short bowel syndrome. The Journal of Pediatrics. http://dx.doi.org/10.1016/j.jpeds.2016.10.027 pii: S0022–3476(16)31095-2.

[19] Drucker, D.J., Yusta, B., 2014. Physiology and pharmacology of the enteroendocrine hormone glucagon-like peptide-2. Annual Review of Physiology 76:561–583.

[20] Bahrami, J., Yusta, B., Drucker, D.J., 2010. ErbB activity links the glucagon-like peptide-2 receptor to refeeding-induced adaptation in the murine small bowel. Gastroenterology 138(7):2447–2456.

[21] Lee, S.-J., Lee, J., Li, K.K., Holland, D., Maughan, H., Guttman, D.S., et al., 2012. Disruption of the murine Glp2r impairs Paneth cell function and increases susceptibility to small bowel enteritis. Endocrinology 153(3):1141–1151.

[22] Scrocchi, L.A., Brown, T.J., MacLusky, N., Brubaker, P.L., Auerbach, A.B., Joyner, A.L., et al., 1996. Glucose intolerance but normal satiety in mice with a null mutation in the glucagon-like peptide receptor gene. Nature Medicine 21: 254–258.

[23] Broer, A., Juelich, T., Vanslambrouck, J.M., Tietze, N., Solomon, P.S., Holst, J., et al., 2011. Impaired nutrient signaling and body weight control in a Na+ neutral amino acid cotransporter (Slc6a19)-deficient mouse. Journal of Biological Chemistry 286(30):26638–26651.

[24] Efeyan, A., Comb, W.C., Sabatini, D.M., 2015. Nutrient-sensing mechanisms and pathways. Nature 517(7534):302–310.

[25] Gingras, A.C., Kennedy, S.G., O'Leary, M.A., Sonenberg, N., Hay, N., 1998. 4E-BP1, a repressor of mRNA translation, is phosphorylated and inactivated by the Akt(PKB) signaling pathway. Genes & Development 12(4):502–513.

[26] Shin, E.D., Estall, J.L., Izzo, A., Drucker, D.J., Brubaker, P.L., 2005. Mucosal adaptation to enteral nutrients is dependent on the physiologic actions of glucagon-like Peptide-2 in mice. Gastroenterology 128(5):1340–1353.

[27] Guertin, D.A., Sabatini, D.M., 2007. Defining the role of mTOR in cancer. Cancer Cell 12(1):9–22.

[28] Guan, X., Stoll, B., Lu, X., Tappenden, K.A., Holst, J.J., Hartmann, B., et al., 2003. GLP-2-mediated up-regulation of intestinal blood flow and glucose uptake is nitric oxide-dependent in TPN-fed piglets. Gastroenterology 125(1): 136–147.

[29] Burrin, D.G., Stoll, B., Jiang, R., Petersen, Y., Elnif, J., Buddington, R.K., et al., 2000. GLP-2 stimulates intestinal growth in premature TPN-fed pigs by suppressing proteolysis and apoptosis. American Journal of Physiology-Gastrointestinal and Liver Physiology 279(6):G1249–G1256.

[30] Niinikoski, H., Stoll, B., Guan, X., Kansagra, K., Lambert, B.D., Stephens, J., et al., 2004. Onset of small intestinal atrophy is associated with reduced intestinal blood flow in TPN-fed neonatal piglets. The Journal of Nutrition 134(6): 1467–1474.

[31] Bjerknes, M., Cheng, H., 2001. Modulation of specific intestinal epithelial progenitors by enteric neurons. Proceedings of the National Academy of Sciences Unites States of America 98(22):12497–12502.

[32] Guan, X., Karpen, H.E., Stephens, J., Bukowski, J.T., Niu, S., Zhang, G., et al., 2006. GLP-2 receptor localizes to enteric neurons and endocrine cells expressing vasoactive peptides and mediates increased blood flow. Gastroenterology 130(1):150–164.

[33] Lundgren, O., Jodal, M., Jansson, M., Ryberg, A.T., Svensson, L., 2011. Intestinal epithelial stem/progenitor cells are controlled by mucosal afferent nerves. PLoS One 6(2):e16295.

[34] Mourad, F.H., Saade, N.E., 2011. Neural regulation of intestinal nutrient absorption. Progress in Neurobiology 95(2):149–162.

[35] Foley, M.K., Inoue, Y., Souba, W.W., Sarr, M.G., 1998. Extrinsic innervation modulates canine jejunal transport of glutamine, alanine, leucine, and glucose. Surgery 123(3):321–329.

[36] Zoncu, R., Bar-Peled, L., Efeyan, A., Wang, S., Sancak, Y., Sabatini, D.M., 2011. mTORC1 senses lysosomal amino acids through an inside-out mechanism that requires the vacuolar H(+)-ATPase. Science 334(6056):678–683.

[37] Ohanna, M., Sobering, A.K., Lapointe, T., Lorenzo, L., Praud, C., Petroulakis, E., et al., 2005. Atrophy of S6K1(−/−) skeletal muscle cells reveals distinct mTOR effectors for cell cycle and size control. Nature Cell Biology 7(3):286–294.

[38] Nicklin, P., Bergman, P., Zhang, B., Triantafellow, E., Wang, H., Nyfeler, B., et al., 2009. Bidirectional transport of amino acids regulates mTOR and autophagy. Cell 136(3):521–534.

[39] Jiang, Y., Rose, A.J., Sijmonsma, T.P., Broer, A., Pfenninger, A., Herzig, S., et al., 2015. Mice lacking neutral amino acid transporter B(0)AT1 (Slc6a19) have elevated levels of FGF21 and GLP-1 and improved glycaemic control. Molecular Metabolism 4(5):406–417.

[40] Clemmensen, C., Jorgensen, C.V., Smajilovic, S., Brauner-Osborne, H., 2016. Robust GLP-1 secretion by basic L-amino acids does not require the GPRC6A receptor. Diabetes, Obesity and Metabolism. http://dx.doi.org/10.1111/dom.12845.

[41] Clemmensen, C., Smajilovic, S., Smith, E.P., Woods, S.C., Brauner-Osborne, H., Seeley, R.J., et al., 2013. Oral L-arginine stimulates GLP-1 secretion to improve glucose tolerance in male mice. Endocrinology 154(11):3978–3983.

[42] Meek, C.L., Lewis, H.B., Vergese, B., Park, A., Reimann, F., Gribble, F., 2016. The effect of encapsulated glutamine on gut peptide secretion in human volunteers. Peptides 77:38–46.

[43] Samocha-Bonet, D., Wong, O., Synnott, E.L., Piyaratna, N., Douglas, A., Gribble, F.M., et al., 2011. Glutamine reduces postprandial glycemia and augments the glucagon-like peptide-1 response in type 2 diabetes patients. The Journal of Nutrition 141(7):1233–1238.

[44] Greenfield, J.R., Farooqi, I.S., Keogh, J.M., Henning, E., Habib, A.M., Blackwood, A., et al., 2009. Oral glutamine increases circulating glucagon-like peptide 1, glucagon, and insulin concentrations in lean, obese, and type 2 diabetic subjects. The American Journal of Clinical Nutrition 89(1):106–113.

[45] Wang, W.W., Qiao, S.Y., Li, D.F., 2009. Amino acids and gut function. Amino Acids 37(1):105–110.

[46] Dube, P.E., Forse, C.L., Bahrami, J., Brubaker, P.L., 2006. The essential role of insulin-like growth factor-1 in the intestinal tropic effects of glucagon-like peptide-2 in mice. Gastroenterology 131(2):589–605.

[47] Yusta, B., Holland, D., Koehler, J.A., Maziarz, M., Estall, J.L., Higgins, R., et al., 2009. ErbB signaling is required for the proliferative actions of GLP-2 in the murine gut. Gastroenterology 173(3):986–996.

[48] Nguyen, H.T., Dalmasso, G., Torkvist, L., Halfvarson, J., Yan, Y., Laroui, H., et al., 2011. CD98 expression modulates intestinal homeostasis, inflammation, and colitis-associated cancer in mice. The Journal of Clinical Investigation 121(5):1733–1747.

[49] Jacobsen, S.H., Olesen, S.C., Dirksen, C., Jorgensen, N.B., Bojsen-Moller, K.N., Kielgast, U., et al., 2012. Changes in gastrointestinal hormone responses, insulin sensitivity, and beta-cell function within 2 weeks after gastric bypass in non-diabetic subjects. Obesity Surgery 22(7):1084–1096.

[50] Cazzo, E., Pareja, J.C., Chaim, E.A., Geloneze, B., Barreto, M.R., Magro, D.O., 2016. GLP-1 and GLP-2 levels are correlated with satiety regulation After Roux-en-Y gastric bypass: results of an exploratory prospective study. Obesity Surgery. http://dx.doi.org/10.1007/s11695-016-2345-3.

[51] Salehi, M., D'Alessio, D.A., 2016. Mechanisms of surgical control of type 2 diabetes: GLP-1 is the key factor-maybe. Surgery for Obesity and Related Diseases 12(6):1230–1235.

[52] Bojsen-Moller, K.N., Jacobsen, S.H., Dirksen, C., Jorgensen, N.B., Reitelseder, S., Jensen, J.E., et al., 2015. Accelerated protein digestion and amino acid absorption after Roux-en-Y gastric bypass. The American Journal of Clinical Nutrition 102(3):600–607.

[53] Khoo, C.M., Muehlbauer, M.J., Stevens, R.D., Pamuklar, Z., Chen, J., Newgard, C.B., et al., 2014. Postprandial metabolite profiles reveal differential nutrient handling after bariatric surgery compared with matched caloric restriction. Annals of Surgery 259(4):687–693.

